Equilibrium Charge States of Br and I Ions in Solids and Gases in the Energy Range 10–180 MeV*

C. D. Moak, H. O. Lutz,† L. B. Bridwell,‡ L. C. Northcliffe,§ and S. Datz

Oak Ridge National Laboratory, Oak Ridge, Tennessee

(Received 24 July 1968)

Monoenergetic bromine and iodine ions from the Oak Ridge tandem accelerator and an MP tandem accelerator have been used to investigate the variations of ionic charge states with various gaseous and solid target materials. In these measurements, beams containing a single charge state and energy were obtained by magnetic analysis and passed through solid targets or windowless gas targets before passing through an electrostatic analyzer. The electrostatic analyzer was fitted with a position-sensitive silicon surface-barrier detector. The most probable charge states are compared with the general relationships given by Dmitriev and Nikolaev. Strongly non-Gaussian distributions have been found at certain energies; most of these irregularities have been associated with ionic shell effects and with multiple ionization.

INTRODUCTION

THE availability of heavy ion beams of accurately known energy and mass (or nuclear charge) has brought about renewed interest in the interaction of these heavy ions with matter. Of particular interest is the dependence of the ionic charge states on the state of condensation of the material, and how the degree of ionization influences the energy losses by heavy ions. Bohr's original theory on heavy-ion stopping power[1] predicts that the stopping power for ions at a given velocity depends quadratically on the mean charge carried by the ion. The more recent theory of Lindhard *et al.*[2] yields a dependence on the nuclear charge alone and not on the state of ionization.

Matters of practical interest such as accelerator design, beam intensity measurement, and direct nuclear-electrical energy conversion require a knowledge of the ionic charge states as a function of ion energy. Most of the previous experimental work has been done using heavy ions that are less massive than Ar. Some of the work dealing with solid media is described in Refs. 3–8. Some of the first charge-state work done with ions as heavy as fission fragments was reported by Lassen,[9,10] Almqvist *et al.*,[11] and Litherland *et al.*[12] report some charge-state data for ^{79}Br and ^{127}I in carbon foils.

Lassen has shown that differences exist between the average charge states of heavy ions emerging from gases and solids and that, for gases, the average charge increases with density.[10] This density effect has been attributed to the increase in ionization probability from excited states with decrease in time between collisions.[13] The effect of ionic shell structure upon equilibrium charge distributions has been reported.[14–17] Small deviations from Gaussian-shaped charge distributions have been shown to be due to multiple electron-loss events.[18]

EXPERIMENTAL PROCEDURE

The experimental arrangement is shown in Fig. 1. Single component beams of ^{79}Br and ^{127}I were obtained from the Oak Ridge tandem accelerator and an MP tandem accelerator.[19] Ions with a specific value of ME/q^2 were selected by the 90° analyzer magnet and transmitted to the experimental equipment. Spectra

* Research sponsored by the U.S. Atomic Energy Commission under contract with Union Carbide Corporation.

† Present address: Max Planck Institut für Kernphysik, Heidelberg, Germany.

‡ Present address: Murray State University, Murray, Ky.

§ Present address: Texas A & M University, College Station, Tex.

[1] N. Bohr, Phil. Mag. **25**, 10 (1913).

[2] J. Lindhard, M. Scharff, and H. E. Schiott, Kgl. Danske Videnskab. Selskab, Mat. Fys. Medd. **33**, No. 14 (1963).

[3] V. S. Nikolaev, I. S. Dmitriev, L. N. Fateeva, and Ya. A. Teplova, Zh. Eksperim. i Teor. Fiz. **33**, 1325 (1958) [English transl.: Soviet Phys.—JETP 6, 1019 (1958)].

[4] L. C. Northcliffe, Phys. Rev. **120**, 1744 (1960).

[5] V. S. Nikolaev, I. S. Dmitriev, L. N. Fateeva, and Ya. A. Teplova, Zh. Eksperim. i Teor. Fiz. **39**, 905 (1960) [English transl.: Soviet Phys.—JETP **12**, 627 (1961)].

[6] H. H. Heckman, E. L. Hubbard, and W. G. Simon, Phys. Rev. **129**, 1240 (1963).

[7] F. W. Martin, Phys. Rev. **140**, A75 (1965).

[8] D. L. Bernard, B. E. Bonner, G. C. Phillips, and P. H. Stelson, Nucl. Phys. **73**, 513 (1965).

[9] N. O. Lassen, Phys. Rev. **69**, 137 (1946).

[10] N. O. Lassen, Kgl. Danske Videnskab. Selskab, Mat. Fys. Medd. **26**, No. 5 (1951).

[11] E. Almqvist, C. Broude, M.A. Clark, J. A. Kuehner, and A. E. Litherland, Can. J. Phys. **40**, 954 (1962).

[12] A. E. Litherland, E. Almqvist, R. H. Andrews, C. Broude, and J. A. Kuehner, Bull. Am. Phys. Soc. **8**, 75 (1963).

[13] N. Bohr and J. Lindhard, Kgl. Danske Videnskab. Selskab, Mat. Fys. Medd. **28**, No. 7 (1954).

[14] I. S. Dmitriev and V. S. Nikolaev, Zh. Eksperim. i Teor. Fiz. **47**, 615 (1964) [English transl.: Soviet Phys.—JETP **20**, 409 (1965)].

[15] C. D. Moak, H. O. Lutz, L. B. Bridwell, L. C. Northcliffe, and S. Datz, Phys. Rev. Letters **18**, 41 (1967).

[16] M. S. Moore and L. G. Miller, Phys. Rev. **157**, 1049 (1967).

[17] R. L. Wolke (private communication).

[18] V. S. Nikolaev, Usp. Fiz. Nauk **85**, 679 (1965) [English transl.: Soviet Phys.—Usp. **8**, 269 (1965)].

[19] We are indebted to High Voltage Engineering Corporation, Burlington, Mass., for the use of the MP tandem accelerator.

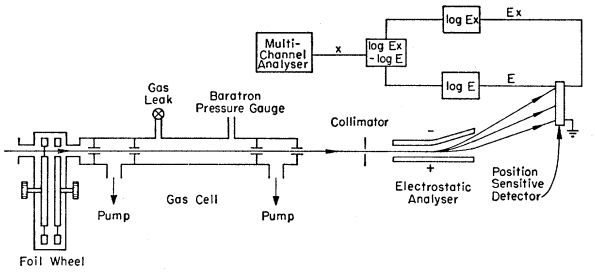

FIG. 1. Experimental arrangement for charge-state measurements with solid or gaseous targets.

were taken with solid and gas targets. Foils of various solid materials were mounted on a foil-wheel arrangement so that targets could be selected without opening the vacuum system. A windowless differentially pumped gas cell was used. The cell consisted of four 1-mm-diam apertures; the spacing between the inner pair of apertures was 50 cm. The differentially pumped regions were made short to eliminate end effects. Cell pressures were measured with a differential manometer,[20] and pressures up to 1.1 Torr were used. The electrostatic analyzer spread the beam until the various emerging charge-state components were spatially separated. A position-sensitive detector of the silicon surface-barrier type[21] was used to detect particles in the separated beam. The operation of the position-sensitive detector is illustrated in Fig. 1. Two pulses, one proportional to Ex (where x is the fractional distance from one end of the detector) and the other proportional to E, the particle energy, were processed in a quotient circuit[22] which yields a pulse which is proportional only to the position x. The position pulse was then fed into a conventional multichannel analyzing system. Using a detector 2 cm in length, position resolution of 0.2 mm was obtained. Simultaneous recording of all charge states eliminated normalization problems. With as many as 17 charge states being recorded in one spectrum, typical peak-to-valley ratios of the dominant charge groups were ≥ 1000. Typical spectra contained $\sim 15\,000$ counts, so that statistical errors in all charge fractions normally were ≤ 0.0037. The width of each charge group, given by the over-all experimental resolution as well as the energy spread in the beam was generally much smaller than the spacing between adjacent groups. In some experiments, a magnetic analyzer was used instead of the electrostatic analyzer. It reduced the positional dispersion due to the energy spread ΔE in the beam thus increasing the resolution. The charge state of the beam coming from the accelerator was always several charges smaller than the most probable charge of an ion which has made many collisions with the target atoms.

Figure 2 shows two representative equilibrium charge distributions obtained by passing a 110-MeV ^{127}I ion beam through 30 Torr cm of H_2 [Fig. 2(a)] or through a carbon foil of 47 μg/cm^2 thickness [Fig. 2(b)]. The abscissa in Fig. 2 gives the deflection of each charge component in the analyzing field; higher charge states appear at higher channel numbers. In the two cases shown, there is a difference of eight charge units between the distribution for a solid and that for a gas. The difference is presumed to be caused by the fact that in dense media, ionic excited states have insufficient time to de-excite before the next collision, whereas in gaseous media ionization must proceed largely from ground states.

RESULTS

For practical applications, it is necessary to know the accurate fraction of ions in a particular charge state after passing the beam through a solid or gaseous stripper. Because of asymmetries in the shapes of the distributions, it is often desirable to use a type of plot which was first introduced by Almqvist *et al.*[11] at Chalk River. The fraction of ions F_q in a particular charge state q is plotted against the energy of the emergent ion; a measured charge distribution appears as a vertical slice through the curves at a constant energy value. Figure 3 shows as an example the energy-dependent equilibrium charge states of ^{79}Br ions in (a) Ar gas, and (b) carbon foils. These and similar data for ^{79}Br in Ne, Ar, Kr, N_2, O_2, SF_6, Be, C, Ni, and UF_4 and for ^{127}I in He, Ne, Ar, Kr, N_2, C, and UF_4 will be made available in the form of tables and full page figures in a forthcoming ORNL report.[23] Data for other target materials not covering the entire energy range will be included.

In order to compare these data with theoretical predictions of the most probable charge of an ion in a medium, we have expressed the measured most probable charges $\bar{q}$ as fractions of the nuclear charge z. These fractions are plotted versus ion velocity v in Figs. 4 and 5. In most cases the charge-state distributions were sufficiently symmetrical to give a clear indication of the most probable charge. For gases, particularly with I ions, the distributions were often complex (cf. Fig. 6) with the result that the definition of most probable charge is vague. In such cases, vertical bars have been inserted in the figures to indicate uncertainty in defining the most probable charge. The curves were obtained through the use of semiempirical relationships given by Dmitriev and Nikolaev.[14] The solid portions of the curves have the form

$$\bar{q}/z=[\ln(v/mz^{\alpha})][\ln(nz^{\beta})]^{-1}, \qquad (1)$$

[20] MKS Instruments, Inc., Burlington, Mass.
[21] Nuclear Diodes, Inc., Prairie View, Ill.
[22] M. G. Strauss and R. Brenner, Rev. Sci. Instr. **36**, No. 12 (1965).
[23] S. Datz, C. D. Moak, H. O. Lutz, L. C. Northcliffe, and L. B. Bridwell, forthcoming Oak Ridge National Laboratory report.

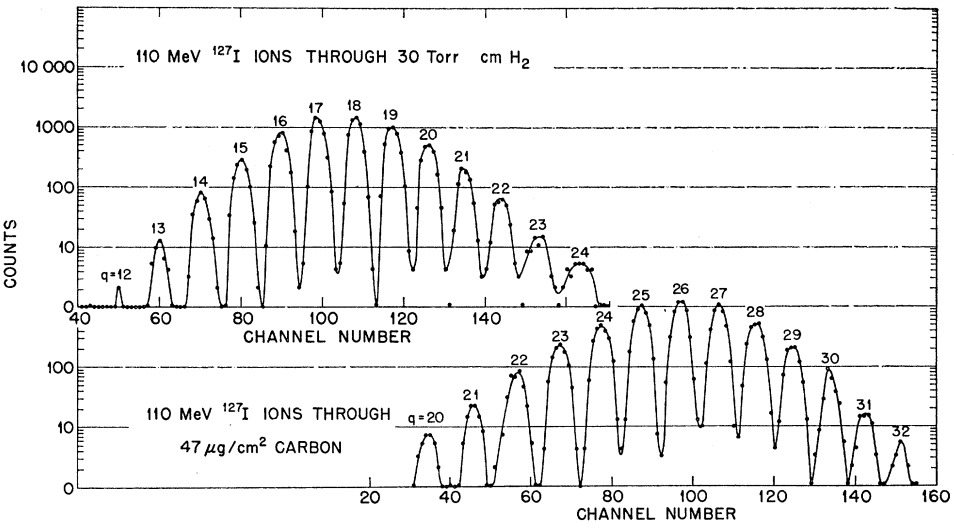

FIG. 2. The condensation effect. The two spectra illustrate the large difference between the charge distributions from gases and solids. The lower spectrum, taken with a higher field setting on the analyzer, has a larger peak spacing; the analyzer was cross-calibrated at $q=20$ for proper charge identification.

where α, m, n, and β are empirical constants. None of the constants appears to depend upon the mass or nuclear charge of the ion. The constants α and β depend only upon the form of the medium (solid or gas); the constants m and n depend rather insensitively ($\pm 30\%$) upon the mass of the target atoms (the values used here are those given for Ar). The range of applicability of Eq. (1) is taken to be $0.3 \leq q/z \leq 0.9$ and below $q/z=0.3$, it is assumed to vary linearly with velocity (see Fig. 5).

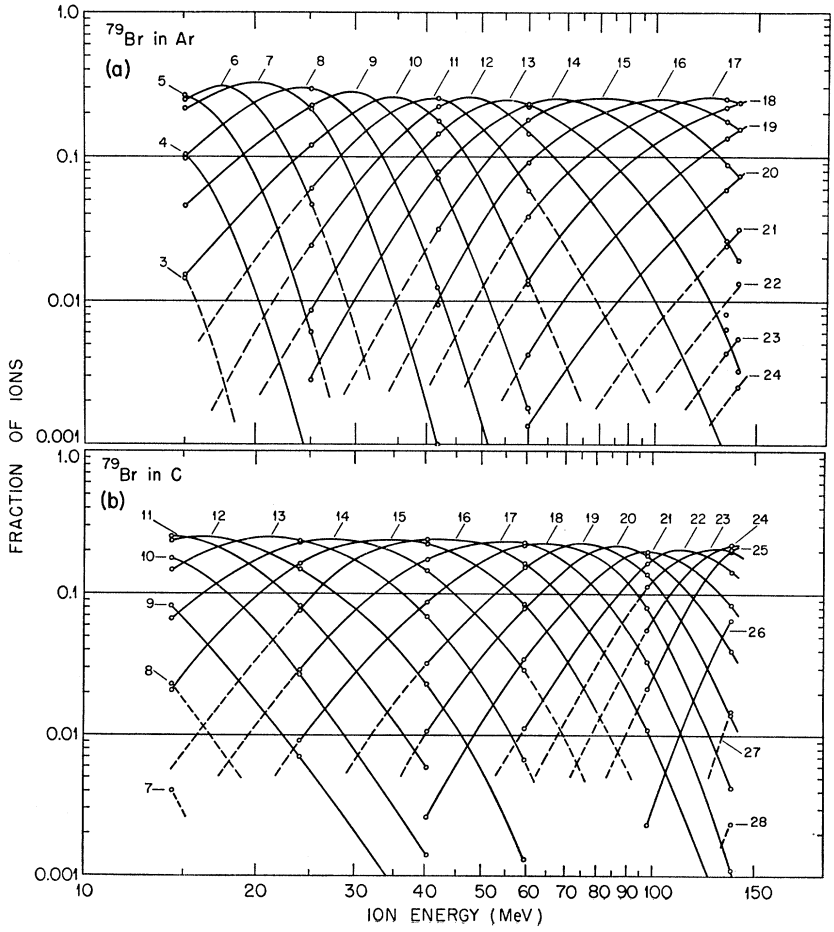

FIG. 3. Fractional population versus energy for various charge states of ^{79}Br in (a) Ar and (b) C. The number on each curve denotes its charge state.

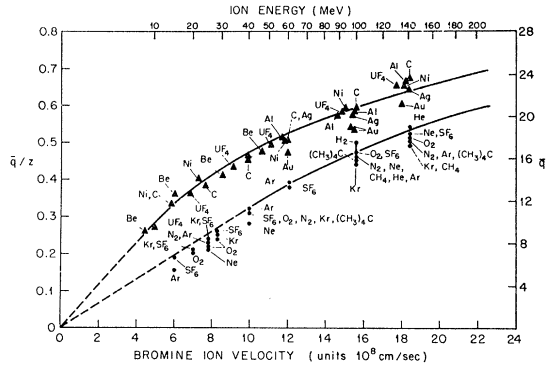

FIG. 4. Most probable charge state expressed as a fraction of nuclear charge for ^{79}Br ions in solids (upper group) and gases (lower group) versus ion velocity for various substances.

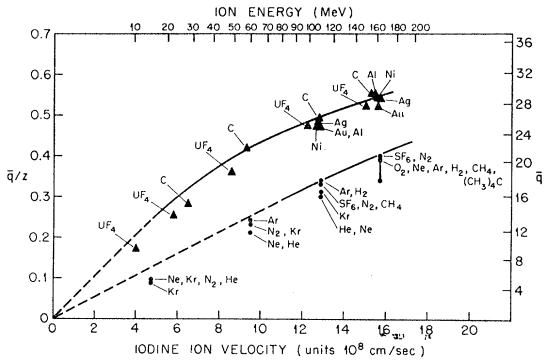

FIG. 5. Most probable charge state expressed as a fraction of nuclear charge for ^{127}I ions in solids (upper group) and gases (lower group) versus ion velocity for various substances.

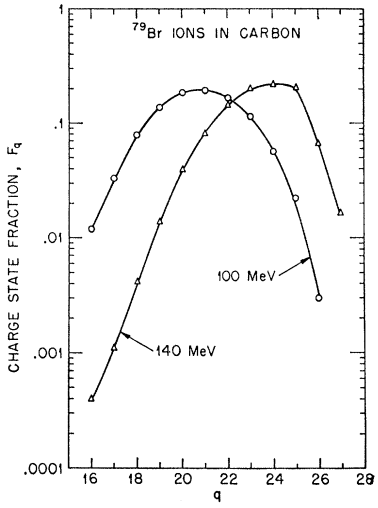

FIG. 7. Charge-state spectrum for ^{79}Br ions in carbon at two bombarding energies.

In the process of data evaluation, one often wishes to extract one or two parameters which fully describe an entire equilibrium charge-state distribution. In many cases, a Gaussian fit to the distribution is not satisfactory, even in energy regions where the resulting charge-state distributions do not come close to $q=0$ or $q=z$ (the nuclear charge of the ion). Figure 6 shows some equilibrium distributions obtained with Br ions [6(a)] and I ions [6(b)] in Ar. The Br ion distributions

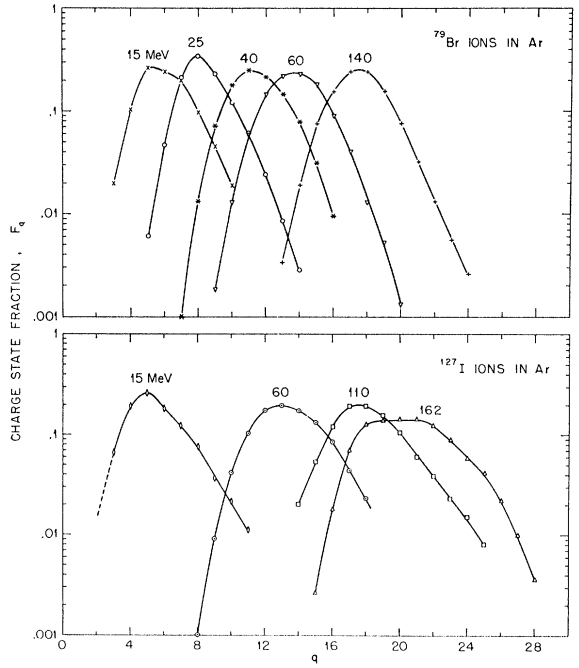

FIG. 6. Some variations in the shapes of charge-state distributions observed for ^{79}Br and ^{127}I ions in Ar.

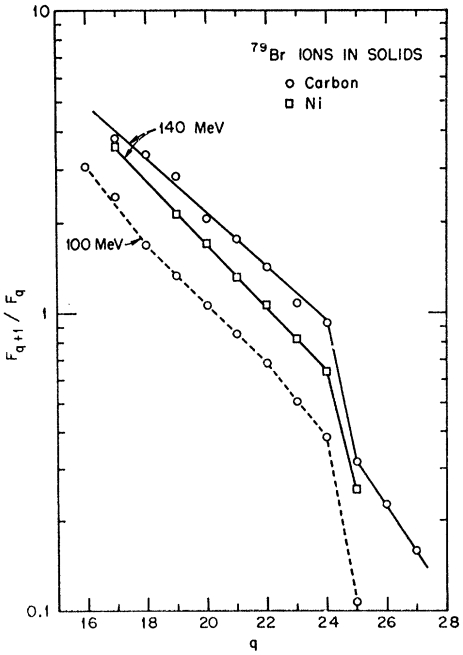

FIG. 8. A discontinuity in the fraction ratio where a shell in the electronic structure of the ion is crossed.

are only slightly asymmetric toward higher population of higher charge states. In the case of I ions the skewness is much more pronounced and at the highest energies (160 MeV) the top of the distribution is flat over four charge states. Figure 7 illustrates another kind of asymmetry which was found for 140-MeV Br ions in solids. The distribution exhibits an effect at charge 25 which is due to the transition from M-shell to L-shell electron removal.

If the logarithm of the ratio of two adjacent charge-state fractions, $\ln(F_{q+1}/F_q)$, is plotted versus the charge q, the dependence is linear for Gaussian distributions.[18] This type of plot is a sensitive indicator of deviations from Gaussian shape. Assuming only single-electron loss and pickup, a plot of $\ln(\sigma_{q,q+1}/\sigma_{q+1,q})$ versus q should also result in a straight line, since at equilibrium $F_{q+1}/F_q=\sigma_{q,q+1}/\sigma_{q+1,q}$. Here, $\sigma_{q,q+1}$ is the single-electron-loss cross section at charge q, and $\sigma_{q+1,q}$ the single-electron-capture cross section at charge $q+1$. A linear dependence of $\ln(\sigma_{q,q+1}/\sigma_{q+1,q})$ on q is obtained for certain functional shapes of the cross sections, e.g., if the capture and loss cross sections in the charge region of the equilibrium distribution can be approximated by exponentials (e^q and e^{-q}, respectively). Figure 8 shows a plot of $\ln(F_{q+1}/F_q)$ versus q for 100- and 140-MeV Br ions passing through C and Ni foils. The discontinuity due to the L-M shell transition is shown more clearly with this type of plot than with that of Fig. 7.

Figure 9 shows a similar plot for I ions in Kr, He, and H_2 at 110, and Kr, Ar, and He at 162 MeV. At both energies, with Ar, the slope expected for a Gaussian distribution changes abruptly at charge 18+ and remains flat to charge 25+ where it breaks again in a downward direction (i.e., the population in charge states 18 to 25, corresponding to $3p$ and $3s$ subshells, are higher than anticipated from a simple picture of charge-changing processes). The same types of distributions were obtained with all target gases except H_2 and He, where the distributions obtained were more symmetric.

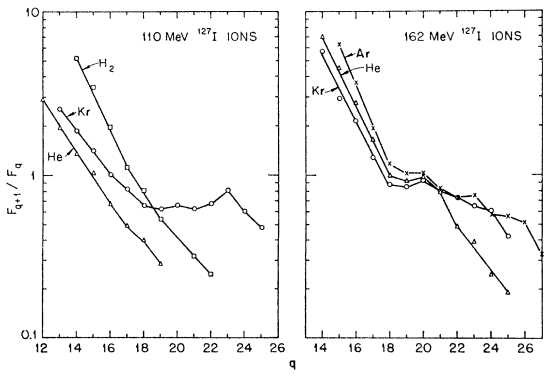

FIG. 9. Fraction-ratio discontinuities due to shell-effects and multiple-electron-loss effects in the ^{127}I ion.

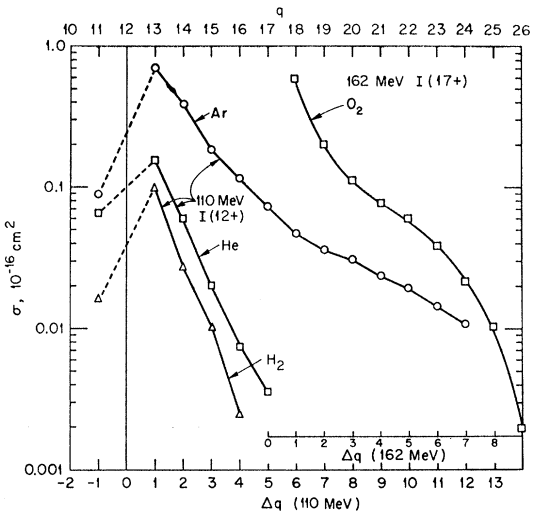

FIG. 10. Charge-changing cross sections for ^{127}I ions from various target gases.

An explanation of these effects may be found in the relatively high probability for multiple-electron loss.[24] In many cases, we have measured nonequilibrium charge distributions for gases to sufficiently low target densities to extract single-collision cross sections (to be published elsewhere). Figure 10 shows measured charge-change cross sections from charge 12+ for 110-MeV I ions in Ar, He, and H_2 and from charge 17+ for 162-MeV I ions in O_2. As many as 12 electrons are frequently removed in a single collision for the case of Ar, and the sum of the multiple-loss cross sections is larger than the single-loss cross section. At a closed shell ($q=25$), the multiple-electron-loss cross section decreases sharply due to a shell transition. This decrease may account for the break in the $\ln(F_{q+1}/F_q)$ curves at $q=25$, Fig. 9.

Less understandable is the break at $q=18$ and the relatively slow decline of the cross-section curve in the region of $q=18$ to $q=25$ ($3p$ and $3s$ subshells). The cross section for removal of 12 electrons from 110-MeV I^{12+} in Ar is only a factor of 5 lower than the cross section for removal of six electrons. This behavior is responsible for the rather flat portion of the $\ln(F_{q+1}/F_q)$ curve of Fig. 9. For the light gases, He and H_2, the data of Fig. 10 indicate comparatively small multiple-loss cross sections and this is reflected in the fact that the $\ln(F_{q+1}/F_q)$ curves for He and H_2 (Fig. 9) show a much smaller flat portion in the range $q>18$. We infer from these data that multiple-electron loss must require that the target atom have large atomic number.

[24] S. Datz, C. D. Moak, H. O. Lutz, L. C. Northcliffe, and L. B. Bridwell, in *Proceedings of the Fifth International Conference on the Physics of Electronic and Atomic Collisions* (Publishing House Nauka, Leningrad, USSR, 1967).